

CFD MODELLING OF PARTIALLY BAFFLED AGITATED VESSELS WITH FREE SURFACES

Jean-Philippe TORRÉ¹, David F. FLETCHER², Thierry LASUYE³, Catherine XUEREB¹

¹ Laboratoire de Génie Chimique CNRS UMR 5503, 5 rue Paulin Talabot, 31106 Toulouse, France.

² School of Chemical and Biomolecular Engineering, The University of Sydney, NSW 2006, Australia

³ LVM Quality and Innovation Department, Usine de Mazingarbe,
Chemin des Soldats, 62160 Bully Les Mines, France

ABSTRACT

Whilst the use of CFD to study mixing vessels is now commonplace, there are still many specialised applications that are yet to be addressed. Here we present CFD and PIV results for a partially baffled vessel with a free surface. We show that there are significant transient effects that mean many of the “rules of thumb” that have been developed for fully-baffled vessels must be revisited. In particular such flows have central vortices that are unsteady and complex, transient flow structures generated by the impeller-baffle interactions.

INTRODUCTION

Mixing is one of the most common and most important operations in the process industries. The situation most frequently encountered in industry is an agitated vessel which is fully-baffled, causing the destruction of the impeller-generated vortex and thus having a flat liquid surface. The category of systems represented by stirred baffled tanks that are equipped with baffles but where the baffling effect is not sufficient to prevent vortex formation is called partially-baffled systems. Although partially-baffled reactors are frequently encountered in the polymer, pharmaceutical and specialty chemicals industries, they have been poorly studied in the literature, with an important lack of numerical studies. As a consequence, the computational study of the hydrodynamics which develops in these stirred tanks, where the free surface deformation cannot be neglected, is particularly interesting and challenging.

Extensive literature reviews of experimental and CFD simulation work have been provided for fully baffled vessels (see Brucato *et al.* (1998)), with a great number of these works concentrated on turbulent, single phase flows in tanks stirred by Rushton turbines. In addition, most experimental studies have been carried out with the liquid surface covered by a lid to prevent vortex formation. The unbaffled case, in comparison with baffled vessels, has been much less well studied. Only three studies were found in the literature that are related to the computation of a turbulent flow in a stirred vessel, including a free surface deformation. Ciofalo *et al.* (1996) presented numerical simulations of the free surface profile for unbaffled tanks agitated by a Rushton turbine and a paddle

impeller. The authors developed an iterative method, used with a treatment of non-orthogonal body fitted grids, that allowed prediction of the vortex shape. This was found to be in good agreement with Nagata's theory (1975) and with vortex height experiments conducted in a model tank. In the two other papers, an interface capturing scheme based on the Volume-of-Fluid (VOF) method, reported by Hirt and Nichols (1981), was used to predict the free surface shape. Serra *et al.* (2001) simulated a wavy free surface for a baffled CSTR using VOF in a fully transient simulation of the flow field. Haque *et al.* (2006) carried out numerical simulation of the turbulent flow with a free surface vortex in unbaffled vessels agitated by a paddle impeller and a Rushton turbine.

In previous papers by the present authors, it was demonstrated that a steady, Eulerian-Eulerian multiphase method can predict the vortex shape in good agreement with experimental data for different agitator rotation speeds (Torre *et al.* (2006a)). In addition, the same method was applied in Torre *et al.* (2006b) to compute the free surface shape evolution during agitator stopping. However, no comparisons between the flow-field predictions and experimental data were reported. The study presented here examines the capability of this inhomogeneous multiphase flow CFD approach to capture the free surface shape and the hydrodynamics of a partially-baffled agitated vessel, where the free surface deformation cannot be neglected and the flow is transient.

The flow fields obtained from the computations need to be averaged in time for comparison with the PIV data. This process has highlighted several important questions concerning the time required before averaging can be started and how many agitator rotations are necessary to obtain relevant numerical data. The answers to these questions have proved to be complex, so in the first part of this study guidelines are obtained using single phase simulations for a case where the surface is flat. These are then compared with results from the inhomogeneous model. Then, the capability of the methods used to model partially baffled systems is examined through comparisons between experimental PIV results and CFD numerical predictions.

EXPERIMENTAL APPARATUS

The stirred tank investigated is a partially baffled pilot reactor, equipped with a three bladed retreat curve bottom-entering impeller and two beaver-tail baffles. It was specially designed for allowing PIV measurements in geometries found in real industrial applications. The cylindrical vessel is placed inside a transparent square tank filled with deionised water in order to minimize shell curvature and refraction problems at the cylindrical surface of the inner vessel. The installation is presented in Figure 1 and all the geometrical dimensions are summarized in Table 1.

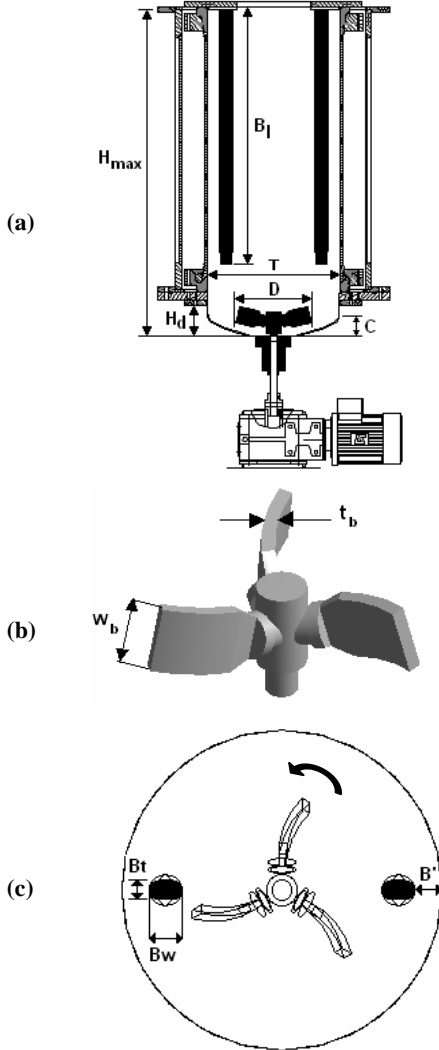


Figure 1: (a) side view of the mixing vessel; (b) details of the agitator; (c) plan view of the mixing vessel

The flow in the stirred vessel was investigated using the Particle Image Velocimetry (PIV) technique. The principles of PIV have been covered in many papers. The reader is referred to Adrian (1991), La Fontaine and Shepherd (1996), Willert and Gharib (1991) for details and Mavros (2001) for a review of the subject. The instantaneous velocity fields were measured in the agitated vessel described above, filled with 109 litres of tap water for all experiments.

	Symbol	Value
Tank diameter	T	450 mm
Maximum tank height	H_{max}	1156 mm
Bottom dish height	H_d	122.9 mm
Agitator diameter	D	260 mm
Number of agitator blades	n_b	3
Agitator blade width	w_b	58 mm
Agitator blade thickness	t_b	9 mm
Agitator retreat angle	θ	15°
Agitator clearance	C	47.2 mm
Baffles length	B_l	900 mm
Number of baffles	n_B	2
Baffle width	B_w	46 mm
Baffle thickness	B_t	27 mm
Distance baffle – reactor shell	B'	38.5 mm
Water height	H	700 mm

Table 1: Dimensions of the agitated vessel studied

The flow was seeded with fluorescent tracer particles of Rhodamine-B provided by Microparticles GmbH (excitation/emission wavelengths: 575 nm/584 nm, fluorochromes incorporated in a PMMA matrix, 1 μm < diameter < 20 μm). A double pulsed Milite Nd:YAG continuum laser at 532 nm (green) was used to illuminate these particles with a short time difference. An appropriate lens and optical system allowed transformation of the laser beam into a vertical laser sheet of 100 mm height and about 1 mm thickness passing through the centre of the vessel and midway between the two baffles.

To capture the frames exposed by laser pulses, a black and white CCD camera (La Vision Imager Intense) with a resolution of 1376 \times 1024 pixels² was used. The camera was equipped with a telephoto lens Nikon – Nikkor 50mm/1.2 used to focus on the laser sheet. It was located 1087 mm away from the light sheet and normal to the jacket sidewall. A high pass filter was placed in front of the camera which enabled capture of light with a wavelength greater than 550 nm, protecting the CCD sensor from unwanted light reflections on gas bubbles and improving contrast. A timing controller was used to link and synchronize the laser and the camera. The image acquisition rate was set to 3 Hz in order not to freeze the flow in the event that low frequency instabilities exist. The snapshots were not synchronized with the passage of impeller blades.

The images were processed using the Davis software package with interrogation cell sizes of 64 pixels for the preliminary step and 32 pixels with 50% overlap for the final step. The concentration of seeded particles was adjusted to have between 5 and 10 particles in each 32 \times 32 pixels² interrogation window. The most probable particle displacement is calculated using a FFT based cross-correlation function to obtain a velocity vector for the considered interrogation window. A radial-axial instantaneous velocity vector map over the whole target area was produced by repeating the cross-correlation for each interrogation area. In each case, 960 images were found to be necessary and sufficient to obtain the averaged flow field.

To cover the entire half tank, the measurements required the construction of a mosaic composed of six different sectors. Each sector measures 80 mm vertically which is smaller than the dimension of the laser sheet to allow optimal intensity in the considered area. Horizontally, each sector covered the entire half tank (225 mm). The sectors were adjusted vertically on specific Y

coordinates to allow 10 mm of superimposition of two adjacent sectors, thus making a junction area. In each junction area, the velocity value considered for the velocity field was the result of the arithmetic average of the two velocities coming from the two adjacent sectors. An irregular glass welding around the vessel led to important light distortions and made it impossible to obtain reliable data acquisition in the vicinity of $Y = 633$ mm. Thus, the area from $Y = 609$ mm to 658 mm has not been considered.

CFD MODELLING

Numerical simulations of the turbulent flow field have been carried out using the commercial CFD package ANSYS-CFX 10.0. The predictions were made in a fully transient manner using fluids at 25°C and the well-known sliding mesh approach. Single phase simulations with only water and a flat free surface were run initially to understand certain elements of the problem before multiphase simulations were run. A novel Eulerian-Eulerian multiphase model which considers the water and air as the continuous and the dispersed phases respectively was developed to allow phase separation and was used to model the free surface deformation. In this inhomogeneous approach, an individual set of continuity and momentum equations was coupled with a homogeneous $k-\epsilon$ turbulence model. The equation system, based on the resolution of the Reynolds Averaged continuity and Navier Stokes equations, is solved in a fully transient manner with assumptions of a constant drag coefficient ($C_D = 0.44$) and a single bubble diameter of 3 mm. The equations of the model and the assumptions used in this study are rigorously detailed in previous papers Torre *et al.* (2006a and b).

The stirred vessel modelled is composed of an unstructured grid of 208,000 and 230,000 nodes for the single and multiphase cases, respectively, optimised by sensitivity studies to be fine enough to capture the flow without being excessive. The rotating part of the vessel was set to be the entire bottom dish which includes the agitator and the sliding interface was represented by the horizontal surface which connects the cylindrical part of the vessel and the bottom dish. A no-slip condition was applied to all walls (vessel and bottom dish walls, agitator and baffles) except the top surface of the vessel where the free-slip condition was set. This boundary condition prevents any flow through the surface and sets the normal gradients for all other quantities to zero. The simulations were carried out with an initial liquid height of 700 mm, and for the inhomogeneous approach with 100 mm of gas above the liquid interface.

The simulations were run using the sliding mesh approach using the transient rotor-stator model available in ANSYS CFX 10.0, with a 2° rotation angle of the agitator per time-step and a maximum of 10 coefficient loops at each time-step. The transient runs were initialized from steady-state results obtained using the Multiple Reference Frame (MRF) approach. The instantaneous velocity of the liquid was monitored during the simulation at fifteen monitor points located on the vertical median plane of the two baffles. These monitor points were located vertically at three different vessel heights ($Y = 200, 400$ and 600 mm) and radially at five positions which are $r = 0, \pm 75$ mm and ± 150 mm.

RESULTS

Single phase simulations

Figure 2 presents the computed velocity at nine of the monitoring-points versus the number of agitator rotations. The velocities measured on the monitor points where $r < 0$ were found to have the same tendencies as those for $r > 0$. Thus, to simplify the figure, only the monitor points with $r > 0$ are presented.

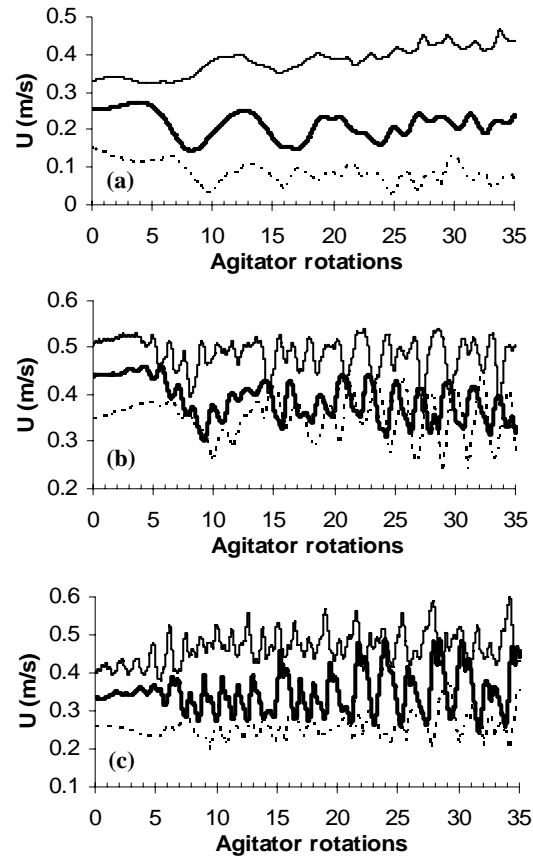


Figure 2: Instantaneous velocity evolution for different locations in the vessel versus agitator rotations. Regular line: $Y = 200$ mm; bold line: $Y = 400$ mm; dashed line: $Y = 600$ mm. (a) $r = 0$; (b) $r = 75$ mm; (c) $r = 150$ mm.

Although the residuals of the momentum, continuity and turbulence equations were all below 10^{-4} , the evolution of the velocity during the first fifteen agitator rotations ($Nr < 15$) differs from the following rotations ($Nr > 15$) for the three vessel heights considered. For $0 < Nr < 5$, the velocity remains quasi-stable with weak oscillations. For $5 < Nr < 15$, a pronounced decrease, followed by an increase of the velocity magnitude for the points located at $r = 0$ and $r = 75$ mm is observed, while this variation is less pronounced for $r = 150$ mm. The reproducibility of the velocity profiles has been tested on two different simulations and it was found to be exactly the same. Thus, the initial agitator rotations were not included in the averaging process and the collection of transient statistics was started only after fifteen revolutions.

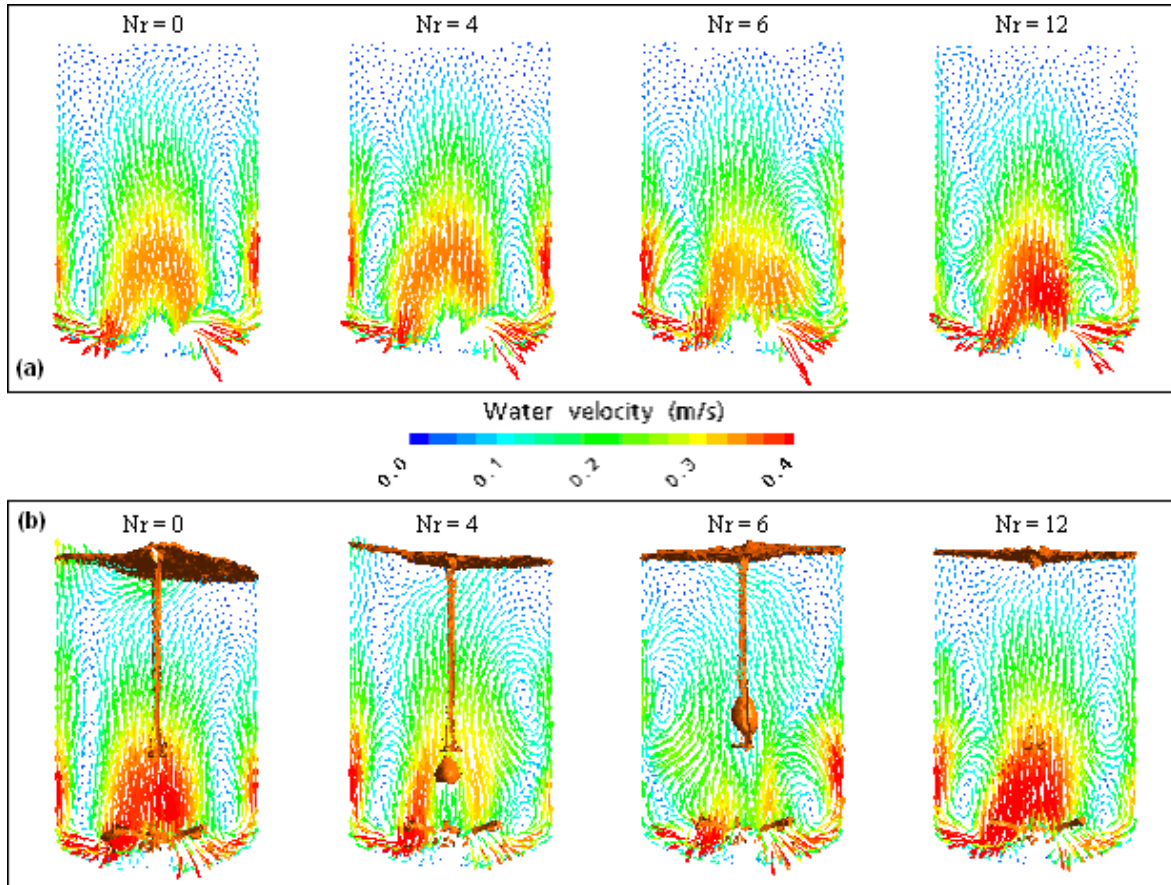
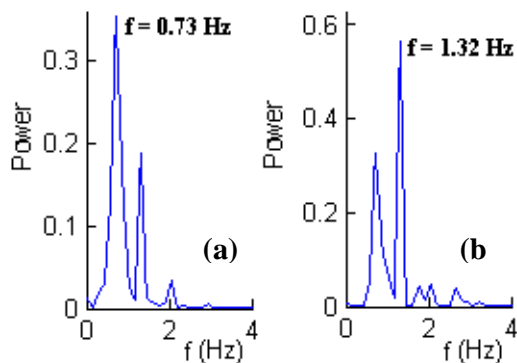


Figure 3: Axial-radial instantaneous velocity vectors on the vertical median plane of the two baffles obtained after steady-state ($Nr = 0$) and at the end of $Nr = 4, 6$ and 12 agitator revolutions: (a) single phase simulation; (b) two phase simulation

Single phase simulations run in steady-state mode (SS) lead to good convergence (residuals $< 10^{-4}$). Contrary to this, the multiphase runs do not converge (residuals between 10^{-4} and 10^{-3}) when the agitator rotation speed was set to a value below 200 rpm. As shown in Figure 3(b), the free surface shape predicted by the inhomogeneous model starts deformed at $Nr = 0$ due to the poor convergence of the steady-state initialisation but



flattens out after a few revolutions.

Figure 4: Fast Fourier Transform power spectrum of the velocity: (a) $Y = 200$ mm, $r = 75$ mm; (b) $Y = 200$ mm, $r = 150$ mm

The predicted flat free surface at 100 rpm is in very good agreement with the experimental observations made at this rotation speed. Figure 3 shows that the SS initialization imposes a double loop flow structure and it takes about five revolutions to break it into multiple secondary recirculation loops. In addition, a Fast Fourier Transform (FFT) spectral analysis of the numerical velocity data obtained from monitor points velocity data during twenty revolutions (from $15 < Nr < 35$) showed a complex, periodic flow structure. The power spectrum is presented in Figure 4 for two example positions and shows characteristic frequencies of 0.73 Hz and 1.32 Hz. The agitator rotation frequency is 1.66 Hz at 100 RPM and thus the intrinsic period of the flow was found not to be an exact multiple of the agitator rotation rate. A period of around two rotations appeared to be the most characteristic, as shown in the vorticity plots.

Figure 5 presents the 10 s^{-1} vorticity isosurface, coloured by the water velocity to highlight the high and low velocity areas. It shows a high vorticity region in the middle of the tank extending from above the agitator to the free surface. When the circumferential velocity is sufficiently high in this region to deform the free surface, a central vortex is formed. The most interesting and unusual feature is the evidence of a swirling vortical structure with filamentous connections of vortices between the rear of the two baffles and the agitator area.

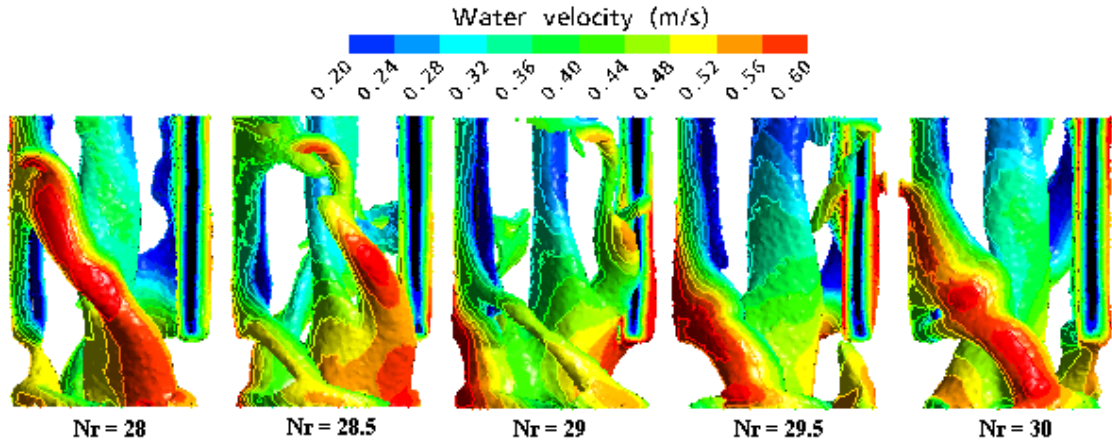


Figure 5: Isosurface of vorticity equal to 10 s^{-1} for the time period covered from the 28th to 30th agitator rotations, coloured by a contour plot of water velocity

These filaments rotate in the vessel in the same sense as the agitator but the global movement was found to have a period of about two agitator revolutions.

This swirling movement which develops with a relative low frequency leads to locally high and low velocity values giving oscillations of the local velocity values, explaining the features observed in Figure 2. This vortical structure confirms the characteristic frequencies obtained by FFT and provides further evidence of the high flow complexity which exists in this partially-baffled system.

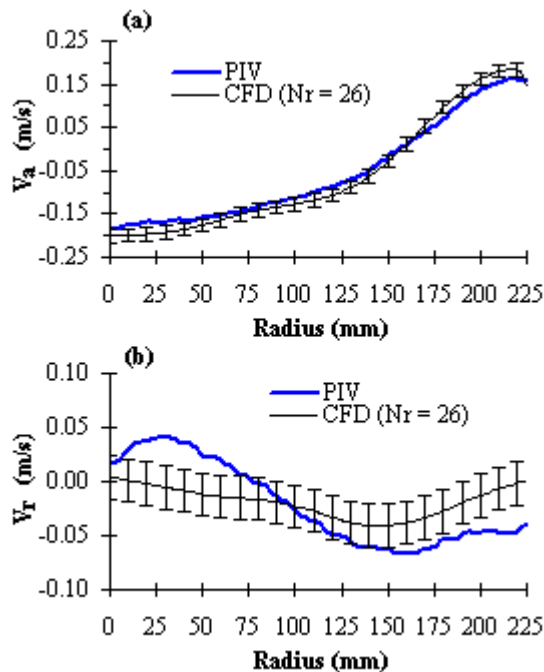


Figure 6: comparison between PIV measurements and CFD numerical predictions: (a) axial velocity $\pm 0.015 \text{ m/s}$; (b) radial velocity $\pm 0.02 \text{ m/s}$

The numerical predictions from the single phase model are compared with experimental data obtained by PIV measurements in Figure 6. The figure presents axial and radial velocity, denoted respectively V_a and V_r , along the entire vessel radius corresponding to a vessel height of $Y = 200 \text{ mm}$ from the bottom dish. The numerical data have been averaged over the fifteenth to thirtieth revolutions and compared with PIV measurement for six different heights. Only one representative comparison is presented in Figure 6 because the conclusions were the same for the different heights tested.

The numerical data have been averaged successively during the agitator rotations to observe how the average develops. The error bars associated with the numerical data represent the fluctuation of the averaged velocity from revolution 22 to 30. It was noted that a stable result was never reached during the averaging process and the velocity changes because of the periodic nature of the flow. Good agreement was obtained with the axial velocity but relatively poor agreement was observed with the radial velocity. The numerical prediction of the averaged radial velocity is very sensitive to the motion of the central vortex. Experimentally, the radial velocity component is very weak compared with the axial and tangential ones, and the central vortex core may explain the deviation observed for $r < 75 \text{ mm}$.

Finally, Figure 7 shows the time-averaged velocity fields obtained for the 100 and 200 rpm cases, obtained using the multiphase model. These show a flow structure which is very close to the original steady-state simulations but with well-converged free surfaces. This is an important result, as it suggests that for industrial purposes it may be sufficient to perform steady-state calculations if only the average flow field is needed. However, the highly transient nature of the flow field is likely to be very important as far as the evolution of mixing times of an injected additive is concerned.

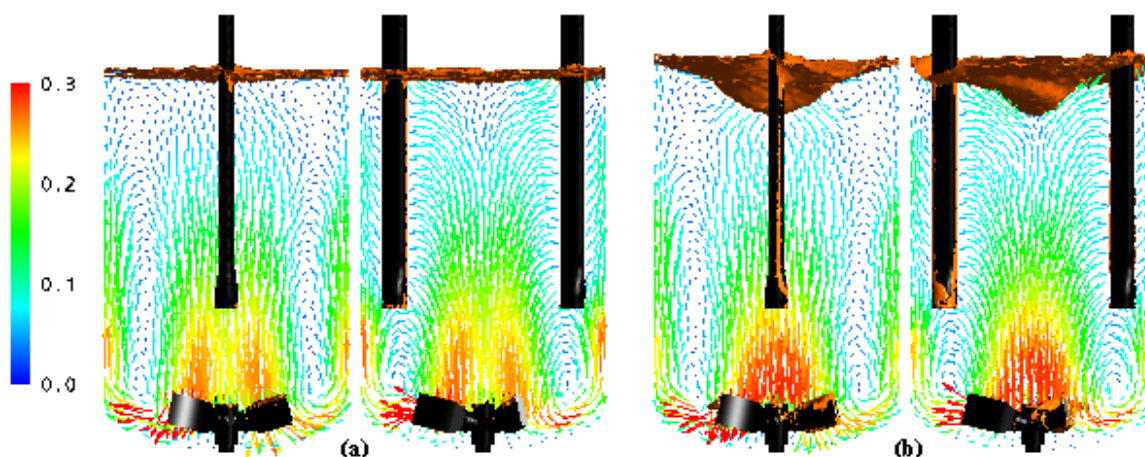


Figure 7: Axial-radial velocity vectors (average velocity from $N_r = 15$ normalized by the tip speed) on the orthogonal baffle plane and on the baffle plane: (a) $N = 100$ RPM, $N_{r,norm} = 12$, $V_{tip} = 1.36$ m/s; (b) $N = 200$ RPM, $N_{r,norm} = 10$, $V_{tip} = 2.72$ m/s

CONCLUSION

A CFD model that can be used to perform transient simulations in partially-baffled mixing vessels with free surfaces has been described. We have shown that at low rotation rates a steady, multiphase simulation does not converge, but that this starting point can be used to obtain transient-averaged data from a converged transient simulation that agree reasonably well with the experimental data. The surprising result is that the system requires simulation of at least five impeller rotations to break down the initial flow pattern and meaningful averaging can only begin after around fifteen revolutions. The time averages show a similar flow structure to the steady-state results but highlight a complex vortical motion with a period of just over two impeller revolution times. The transient model also captures the free surface behaviour well, as the steady-state model does at higher rotation speeds.

The current work is based on the use of the $k-\epsilon$ turbulence model which is known to have limitations when used in transient mode. Future work will investigate the effect of using the Scale-Adaptive Simulation (SAS) model of Menter *et al.* (2003). However for the model to be useful in the design of mixing systems the convergence times and computer requirements must remain practical.

ACKNOWLEDGMENTS

Tessenderlo Group and ANRT (CIFRE/ANRT contract No 1727 / 1413582.00) are gratefully acknowledged for financial support. The authors are also grateful to Alain Muller for the technical assistance he provides on the pilot reactor.

REFERENCES

ADRIAN, R. J., (1991). "Particle imaging techniques for experimental fluid mechanics", *Annual Rev. Fluid Mech.*, **23**, 261-304.
 ALCAMO, R., MICALE, G., GRISAFI, F., BRUCATO, A. and CIOFALO, M. (2005), "Large-eddy simulation of turbulent flow in an unbaffled stirred tank driven by a Rushton turbine", *Chem. Eng. Sci.*, **60** (8-9), 2303-2316.

BRUCATO, A., CIOFALO, M., GRISAFI, F. and MICALE, G. (1998), "Numerical prediction of flow fields in baffled stirred vessels: a comparison of alternative modelling approaches", *Chem. Eng. Sci.*, **53** (21), 3653-3684.

CIOFALO, M., BRUCATO, A., GRISAFI, F. and TORRACA, N. (1996), "Turbulent flow in closed and free-surface unbaffled tanks stirred by radial impellers", *Chem. Eng. Sci.*, **51**(14), 3557-3573.

HAQUE, J. N., MAHMUD, T. and ROBERTS, K. J. (2006), "Modeling turbulent flow with free surface in unbaffled agitated vessels", *Ind. Eng. Chem. Res.*, **45**, 2881-2891.

HIRT, C. W. and NICHOLS, B. D. (1981), "Volume of fluid (VOF) method for the dynamics of free boundaries", *J. Comput. Phys.*, **39** (1), 201-225.

LA FONTAINE, R. F. and SHEPHERD, I. C. (1996), "Particle Image Velocimetry applied to a stirred vessel", *Exp. Therm. Fluid Sci.*, **12**, 256-264.

MAVROS, P. (2001), "Flow visualization in stirred vessels, a review of experimental techniques", *Trans. Inst. Chem. Eng.*, **79**(A), 113-127.

MENTER, F. R., KUNTZ, M. and BENDER, R. (2003), "A scale-adaptive simulation model for turbulent flow prediction", *AIAA paper 2003-0767*.

NAGATA, S. (1975), "Mixing: principles and applications", Wiley, New York.

SERRA, A., CAMPOLO, M. and SOLDATI, A. (2001), "Time-dependent finite-volume simulation of the turbulent flow in a free-surface CSTR", *Chem. Eng. Sci.*, **56** (8), 2715-2720.

TORRÉ, J.P., FLETCHER, D.F., LASUYE, T., XUERE, C. (2006a), "An experimental and computational study of the vortex shape in a partially baffled agitated vessel", *submitted to Chem. Eng. Sci.*

TORRÉ, J.P., FLETCHER, D.F., LASUYE, T., XUERE, C. (2006b), "Transient hydrodynamics of a stirred tank during stopping", *Proceedings of the 12th European Conference on mixing*, 27-30 June 2006, Bologna, 551-558.

WILLERT, C. E. and GHARIB, M. (1991), "Digital particle Velocimetry", *Exp. Fluids*, **10**, 181-193.